Dynamics of infectious diseases according to climate change: The Usutu virus epidemics in Vienna

Franz Rubel and Katharina Brugger

Institute for Veterinary Public Health, Department for Farm Animals and Veterinary Public Health, University of Veterinary Medicine Vienna, Veterinärplatz 1, 1210 Vienna, Austria; franz.rubel@vetmeduni.ac.at

Cite as: Rubel, F. and K. Brugger, 2011: *Dynamics infectious diseases according to climate change: The Usutu virus epidemics in Vienna*. In: Game meat hygiene in focus - Microbiology, epidemiology, risk analysis and quality assurance**.** Paulsen, P. et al. (Eds.), Wageningen Academics Publishers, The Netherlands, 173-198.

Dynamics of infectious diseases according to climate change: The Usutu virus epidemics in Vienna

Franz Rubel and Katharina Brugger
Institute for Veterinary Public Health, Department for Farm Animals and Veterinary Public Health, University of Veterinary Medicine Vienna, Veterinärplatz 1, 1210 Vienna, Austria;
franz.rubel@vetmeduni.ac.at

Summary

As an example of the dynamics of infectious diseases in mid-latitudes, so far mainly observed in the subtropics and tropics, we discuss the Usutu virus (USUV) epidemics in Vienna, Austria. The USUV is an arbovirus, which is closely related to the West Nile virus. It caused mass mortalities mainly of blackbirds (*Turdus merula*). Infections of mammalian hosts or humans are rare. The USUV flavivirus persists in a natural transmission cycle between vectors (mosquitoes) and host reservoirs (birds) and leads - once endemic in a population - to periodic outbreaks. Following the recent work of Rubel *et al.* (2008) and Brugger and Rubel (2009), we present an epidemic model to explain the USUV dynamics in Austria. Within the model framework the USUV dynamics is mainly determined by an interaction of bird immunity and environmental temperature. We demonstrate that the USUV model is able to simulate the observations from the dead-bird surveillance 2001-2005. To investigate future scenarios, we entered temperature predictions from five global climate models into the USUV model and also considered four different climate-warming scenarios defined by the Intergovernmental Panel on Climate Change, IPCC (20 different model-scenario combinations). Long-term simulations cover the period 1901-2100. The results indicate that USUV will persist in the host population after the epidemic peak observed in 2003, but the next major outbreak is expected to occur not before 2019. USUV-specific annual blackbird-mortality time series predict that the outbreak frequency increases successively from the beginning to the end of the century. Additionally we calculated the annually averaged basic reproduction number for the period 1901-2100. The latter depict that undetected major outbreaks before 2000 were unlikely, whereas it is likely that the USUV becomes endemic after 2040.

Keywords: arbovirus, basic reproduction number, simulation, epidemic model, global warming

1. Introduction

The incidence and spread of previously tropical infectious diseases considerably increased under the current situation of climate change (Harvell *et al.*, 2002; Pfeffer and Dobler, 2009; Gale *et al.*, 2010) and global animal trade and migration (Pfeffer and Dobler, 2010). As an example of an emerging or re-emerging zoonosis, the temperature dependent dynamics of the Usutu virus (USUV), which was recently investigated by Rubel *et al.* (2008) and Brugger and Rubel (2009), is presented here. USUV was detected the first time outside Africa in 2001 in Austria (Weissenböck *et al.*, 2002). It is a member of the flaviviridae family of the Japanese encephalitis virus complex and closely related to the more common West Nile virus (WNV), dengue virus (DENV), Japanese encephalitis-virus (JEV) and yellow-fever virus (YFV) (Weissenböck *et al.*, 2002). USUV became well-known, because it caused mass mortalities of

blackbirds (*Turdus merula*) in and around the capital city of Austria, Vienna. The established monitoring programme of the University of Veterinary Medicine Vienna confirmed that USUV overwintered in Austria (Chvala *et al.*, 2007). Although the initial number of dead blackbirds was very low in 2001 and 2002, an epidemic peak was observed during the extraordinary hot summer 2003 (Schönwiese *et al.*, 2004). In the meantime, USUV was also observed in other Central European countries such as Switzerland, Hungary (Bakonyi *et al.*, 2007), and Northern Italy (Lelli *et al.*, 2008; Manarolla *et al.*, 2010). Although it was assumed that USUV does not cause severe or fatal disease in humans, in August 2009, two human cases of Usutu virus neuroinvasive infection were documented in Italy (Pecorari *et al.*, 2009; Cavrini *et al.*, 2009).

Arthropod-borne viruses (arboviruses), like USUV, persist in a natural transmission cycle between vectors (here, mosquitoes of the *Culex pipiens* complex) and avian hosts. Once endemic, it might cause periodic disease outbreaks. Rubel *et al.* (2008) developed a new epidemic model for explaining the multi-seasonal dynamics of the USUV infection in Austria. This model considers both the density-dependent seasonal dynamics of mosquitoes and birds and the USUV bird-mosquito infection cycle. The dynamics of the mosquito population and the virus reproduction rate depend strongly on the environmental temperature. Efficient USUV transmission requires warm temperatures (which increase the reproduction and biting rates of mosquitoes and decrease the extrinsic incubation period). To demonstrate the relationship between warm temperatures and USUV, Figure 1 depicts the total number of dead blackbirds associated with USUV infections (period 2001-2005) together with the spatial distribution of the average number of hot days (days with temperature ≥ 30 °C) in Austria. Conspicuously, the emergence of USUV infections is mainly related to those regions

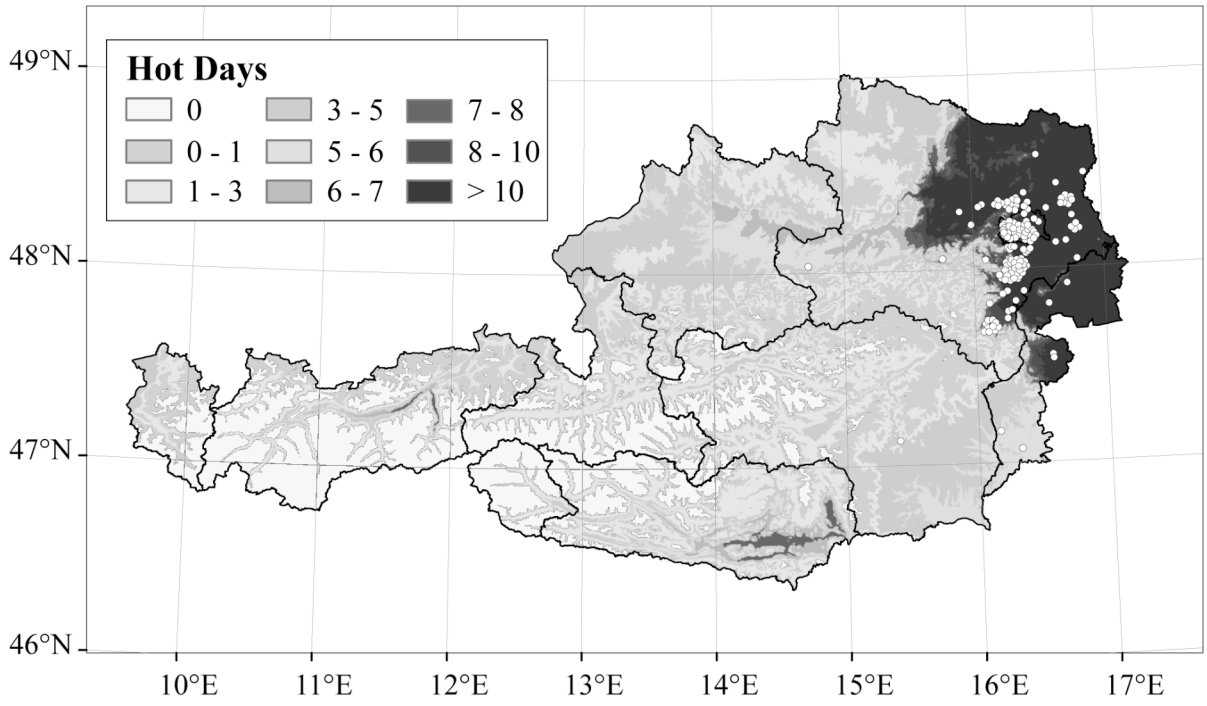

Figure 1: Spatial distribution of the average number of hot days per year in Austria for the climate reference period 1961-1990 (Auer et al., 2001) and blackbirds dead from USUV (white dots; Chvala et al., 2007). Among some other species, about 140 blackbirds dead from USUV infections have been collected between 2001 and 2005.

around Vienna where the number of hot days exceeds 10 days/year. Most of the dead birds were found in the most populated region in the district of Lower Austria, and only few in the surrounding agricultural areas. A more detailed discussion on the dead-bird monitoring is in Weissenböck *et al.* (2003) and Chvala *et al.* (2007).

Here we will respond to the following questions: Is it possible to develop an epidemic model, which can accurately simulate the observed USUV epidemics in Vienna? How might USUV around Vienna develop according to global warming? Should we expect large-scale declines in several bird populations as observed for the related WNV in North America (LaDeau *et al.*, 2007)? To answer the first question, we explain and discuss the USUV model developed by Rubel *et al.* (2008), which calculates (once initialized with some USUV-positive mosquitoes and exclusively forced by environmental temperature) time series of bird and mosquito populations of various health states. It is shown that the epidemic model is able to reproduce the observed numbers of dead birds very well. Therefore, the epidemic model will be forced with long-term climate projections to answer the second and third question.

The applied climate dataset comprises temperature predictions from five different global climate models (GCMs), to incorporate the uncertainty across climate models. However, each GCM was based on the same initial conditions. We used a combination of these five climate models with the four emission scenarios (defined by the Intergovernmental Panel on Climate Change, IPCC) resulting in a total of 20 temperature predictions for the period 2006-2100 to force our USUV model. The results of these multiple model runs are interpreted like results from a stochastic model. Finally, we used temperature observations from a weather station in Vienna to run the USUV model for the period 1901-2005. The major result from the epidemic model runs is a time series of the basic reproduction number of the Usutu virus for the period 1901-2100. It depicts the possibility for a major outbreak as a function of environmental temperature and herd immunity of birds.

2. The epidemic model

Our SEIR (susceptible, exposed, infectious, recovered) model simulates the seasonal lifecycles of blackbirds (*Turdus merula*) and mosquitoes (*Culex pipiens*) and the inter-species USUV infection cycle between birds and mosquitoes (Figure 2). The model has nine compartments (*i.e.* health states): susceptible birds (S_B), latent-infected or exposed birds (E_B), infectious birds (I_B), recovered or immune birds (R_B), dead birds (D_B), mosquito larvae (L_M), susceptible mosquitoes (S_M), latent-infected or exposed mosquitoes (E_M) and infectious mosquitoes (I_M). The movements between health states are defined by 12 parameters, of which seven depend exclusively on the environmental temperature. These are the birth and mortality rates of larvae and (adult) mosquitoes, the infection rates between infectious mosquitoes and susceptible birds and *vice versa* (cross-infection), and the reciprocal of the extrinsic incubation period (here defined as infectivity rate of mosquitoes). Further parameters are the birth rate of birds and the proportion of mosquitos' non-diapausing, which are functions of the Julian calendar day and the geographic latitude. Constant parameters are the mortality rate of birds, the reciprocal of the intrinsic incubation period, and the infectivity rate of birds (*i.e.* the rate of transition within birds from latently infected to infectious), the recovery rate of birds and the death rate of birds. For more details on the mathematical parameter definition see Appendix A. Based on the same initial conditions we used a

combination of these five climate models with the four IPCC emission scenarios resulting in a total of 20 temperature predictions for the period 2006-2100 to force our USUV model. The results of these multiple model runs are interpreted like results from a stochastic model. Finally, we used temperature observations from a weather station in Vienna to run the USUV model for the period 1901-2005. The major results from the epidemic model runs are time series of the basic reproduction number of the health states of birds and mosquitoes, respectively. They depict the possibility for past and future outbreaks as a function of environmental temperature.

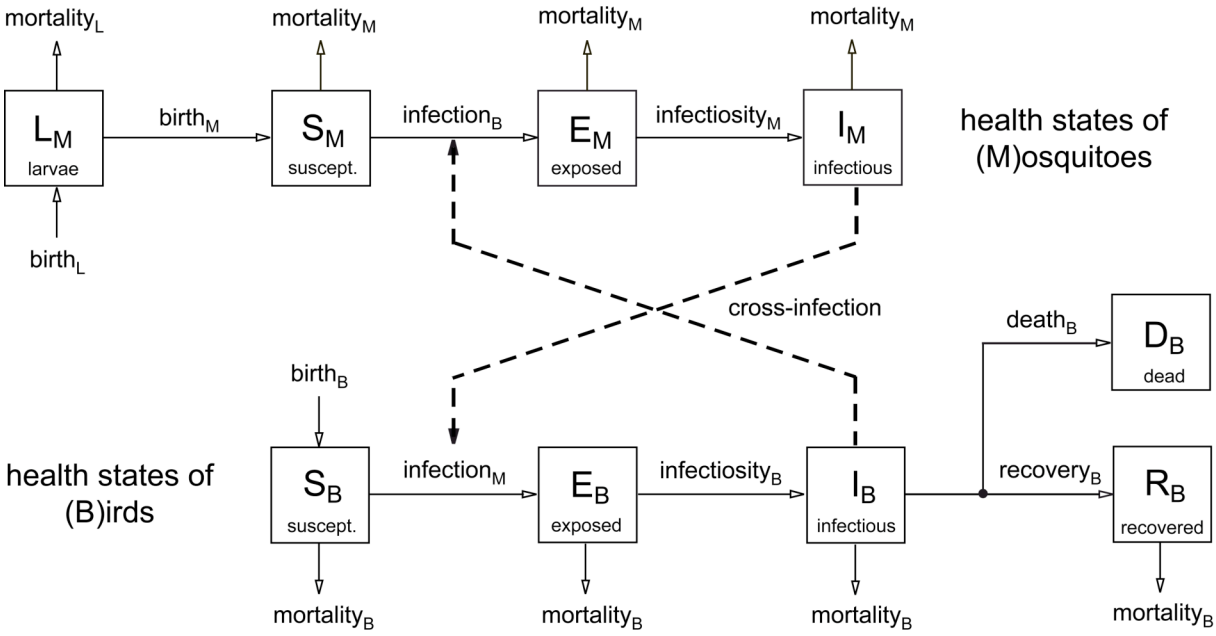

Figure 2: Block diagram of the epidemic model applied to simulate the Usutu virus dynamics in Vienna. The birth and mortality rates of mosquitoes ($birth_L$, $mortality_L$, $birth_M$, $mortality_M$), the infection rates ($infection_B$, $infection_M$) and the infectivity rate of mosquitoes ($infectivity_M$) are considered to be temperature dependent.

In doing so, the numbers of species in specific health state are calculated following the main principle of building budgets. The future number of infectious mosquitoes, for example, is calculated from actually available infectious mosquitoes minus the mosquitoes dying within some specified time step (determined by the $mortality_M$ rate) plus the newly infectious mosquitoes (determined by the $infectivity_M$ rate). Thus, the dynamics of the 9 bird and mosquito health states is mathematically formulated by 9 ordinary differential equations (not shown), which are solved numerically using daily time steps (R source code see Appendix B).

3. Parameter estimation

The extent to which an epidemic model simulates reality depends strongly on the assumed parameters (birth, mortality and transmission rates). Note that the model parameters are generally defined per capita and per day and will be described in detail in the following sub-sections.

3.1 Bird parameters

Because more than 90% of all birds, which died from USUV infections, were blackbirds (*Turdus merula*), we focus on this species. Blackbirds are widespread in woodland, but also one of the most striking birds in urban gardens. Their average life expectancy is about 2 years, but may exceed 20 years in exceptional cases. Knowing the lifetime of blackbirds, the mortality rate can be estimated as its reciprocal value. Hatchwell *et al.* (1996) specified annual mortality rates of 0.34 per year and 0.52 per year in woodland and farmland, respectively. For the land cover of the area around Vienna we applied a mean mortality rate of 0.43 per year corresponding to $mortality_B = 0.0012$ days^{-1}.

In Central Europe blackbirds deposit eggs two to four times per year. Schnack (1991) investigated the breeding success and clutch sizes of blackbirds in 17 city parks in Vienna and in an adjacent lowland forest. On average a clutch size of 4.1 eggs was estimated for the city of Vienna and 4.6 eggs for the woodland. The breeding success (the number of fledged nestlings per eggs laid) was 22.4% for urban blackbirds and 30.7% for forest blackbirds. Similar results were documented by Tomialojc (1993) and Tomialojc (1994) for blackbirds in Poland (mean clutch size of 4.5 eggs, emerging nest losses of 50-92% with mean 68%). On averaged 2.5 young per pair fledged yearly, whereas the most successful pairs reared 8-9 young (Tomialojc, 1994). We assume 2.5 young per pair as bird birth rate. This yields a per capita birth rate of 1.25 per year or $birth_B = 0.00342$ days^{-1}.

Although the mortality rate is assumed to be uniformly distributed over the year, a seasonal cycle was fitted to the observed birth rate. Figure 3 (left) depicts the observed frequency distribution of the blackbird nestlings (bars), as compiled from counts of blackbird clutches in Poland (Tomialojc, 1994), and the fitted theoretical distribution (line). Originally, Tomialojc (1994) published absolute numbers of clutches for two observational periods, which were averaged and shifted by 10 days to account for breeding. As depicted in Figure 3 (left), the distribution is skewed to the right. Therefore, a gamma distribution was selected to describe the observations. By multiplying it with the average annual birth rate, we derived the birth rate as a function of the calendar day as shown in Figure 3 (right).

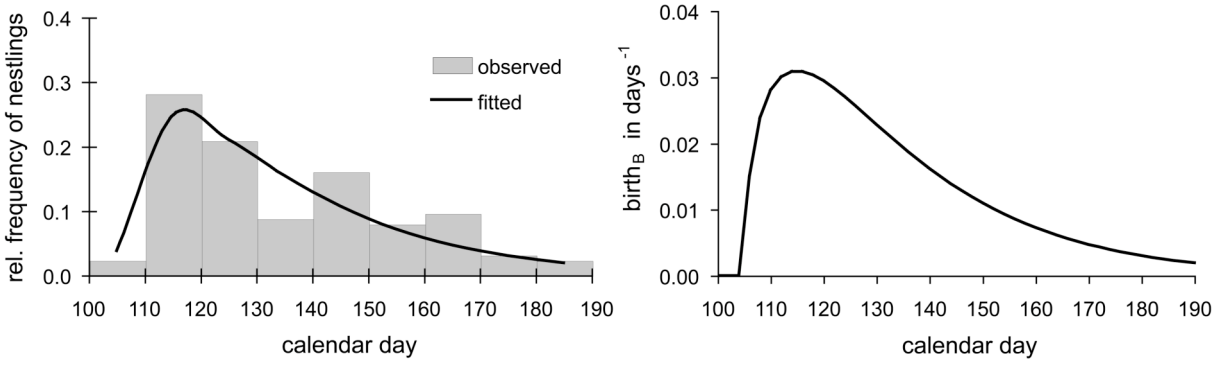

Figure 3: Observed relative frequency of blackbird nestlings (Tomialojc, 1994) with fitted gamma distribution (left) and bird birth rate as function of the Julian calendar day (right).

The breeding density in the city of Vienna varies in the range of 10-210 pairs/km^2 (Schnack, 1991), corresponding to a bird density of 20-420 birds/km^2. Two typical black bird habitats outside the city of Vienna were investigated by Wichmann and Zuna-Kratky (1997). The first habitat is an area covered with vineyards and fallow lands, and the bird density was 77-122

birds/km^2. The second habitat, a mixed forest with embedded grasslands, showed a slightly higher bird density of 104-155 birds/km^2. These densities are much higher than the large-scale blackbird density for central Europe, for example, of 25 birds/km^2 as estimated for the entire region of Germany (Schwarz and Flade, 1989). Considering both the large-scale density and the local densities of favoured blackbird habitats, we assumed an average blackbird density for the area of USUV emergence of about 50 birds/km^2. We used this value to define the carrying capacity of birds.

An accurate estimation of the bird mortality due to USUV infections is difficult. From the data of the dead-bird surveillance we estimated that about 30% of the infected blackbirds died (Weissenböck *et al.*, 2002).

3.2 Temperature-dependent transmission parameters

According to the cross-infection process depicted in Figure 2, two transmission parameters, the forces of infection, must be determined. Here, the forces of infection are abbreviated by the terms $infection_B$ and $infection_M$, which are functions of the mosquito biting rate k and the probabilities p_B and p_M that the USUV is transmitted by a bite. As for WNV, *Culex* mosquitoes are mainly responsible for USUV transmission. On average these mosquitoes are biting every 1-5 days, corresponding to biting rates of k = 0.2-1 days^{-1}; see for example the overview given by Cruz-Pacheco *et al.* (2005). Temporal changes in the effectiveness of transmission essentially delineate the seasonality of WNV and USUV activity and are triggered by the environmental temperature. For a description of this process, the temperature dependence of the duration of the gonotrophic cycle (*i.e.* the development cycle of mosquitoes comprising blood meal as well as development and deposition of eggs) as presented by Reisen *et al.* (2006) was used. The function describing the biting (*i.e.* contact) rate was fitted to the reciprocal of the duration of the mosquito gonotrophic cycle (Rubel *et al.*, 2008). The functional relationship is similar to Figure 4a, because the birth rate of the larvae ($birth_L$) is assumed to be a multiple of the biting rate k. The biting rate increases with increasing temperature according to a logistic function. The infection rates are proportional to the product of the biting rate and the transmission probabilities. Typical WNV probabilities as proposed by various authors vary of 0.02-0.24 (virus transmission by infectious birds to susceptible mosquitoes) and 0.8-1.0 (virus transmission by infectious mosquitoes). We determined the unknown transmission probabilities of USUV by fitting the model to observations, resulting in a transmission probability by infectious birds of $p_B = 0.125$ and by infectious mosquitoes of $p_M = 1.0$ (both are within the range given for WNV).

3.3 Temperature-dependent mosquito parameters

The temperature dependence of mosquito birth and mortality rates (of both larvae and adult mosquitoes) was investigated mainly in the 1960s and 1970s. Unfortunately, most of these studies do not provide functions as required for process models. Therefore, one of our goals was to find general functions describing the relationship between mosquito population parameters and environmental temperature. A selection of functions fitted to data sets published by various authors is depicted in Figure 4.

Figure 4a shows the birth rate of larvae $birth_L$, a synonym for the egg-deposition rate, which is modelled by the scaled reciprocal of the gonotrophic cycle after Reisen *et al.* (2006). We selected the scaling factor so that the average birth rate $birth_L = 0.537$ days^{-1}, as proposed by Wonham *et al.* (2004), is reached at T = 25 °C. Typical mortality rates of larvae are shown in

Figure 4b, where a function was fitted to data from Bailey and Gieke (1968). Alternative functions (not shown) were used for example by Eisenberg *et al.* (1995) or Shaman *et al.* (2006). Most studies are available for the temperature dependent birth rate of adult mosquitoes $birth_M$ (that is, the development rate of immatures). These studies comprise laboratory experiments for *Culex quinquefasciatus* and *Aedes aegypti* (Rueda *et al.*, 1990), a regression line for *Culex annulirostis* (Rae, 1990) as well as discrete values for *Culex tarsalis* (Reisen, 1995) and for *Culex pipiens molestus* (Olejnícek and Gelbic, 2000). Logistic ions $birth_M$ were fitted to all of these data sets and subsequently were evaluated in sensitivity studies (results not shown). As an example, the function fitted to the data published by Reisen

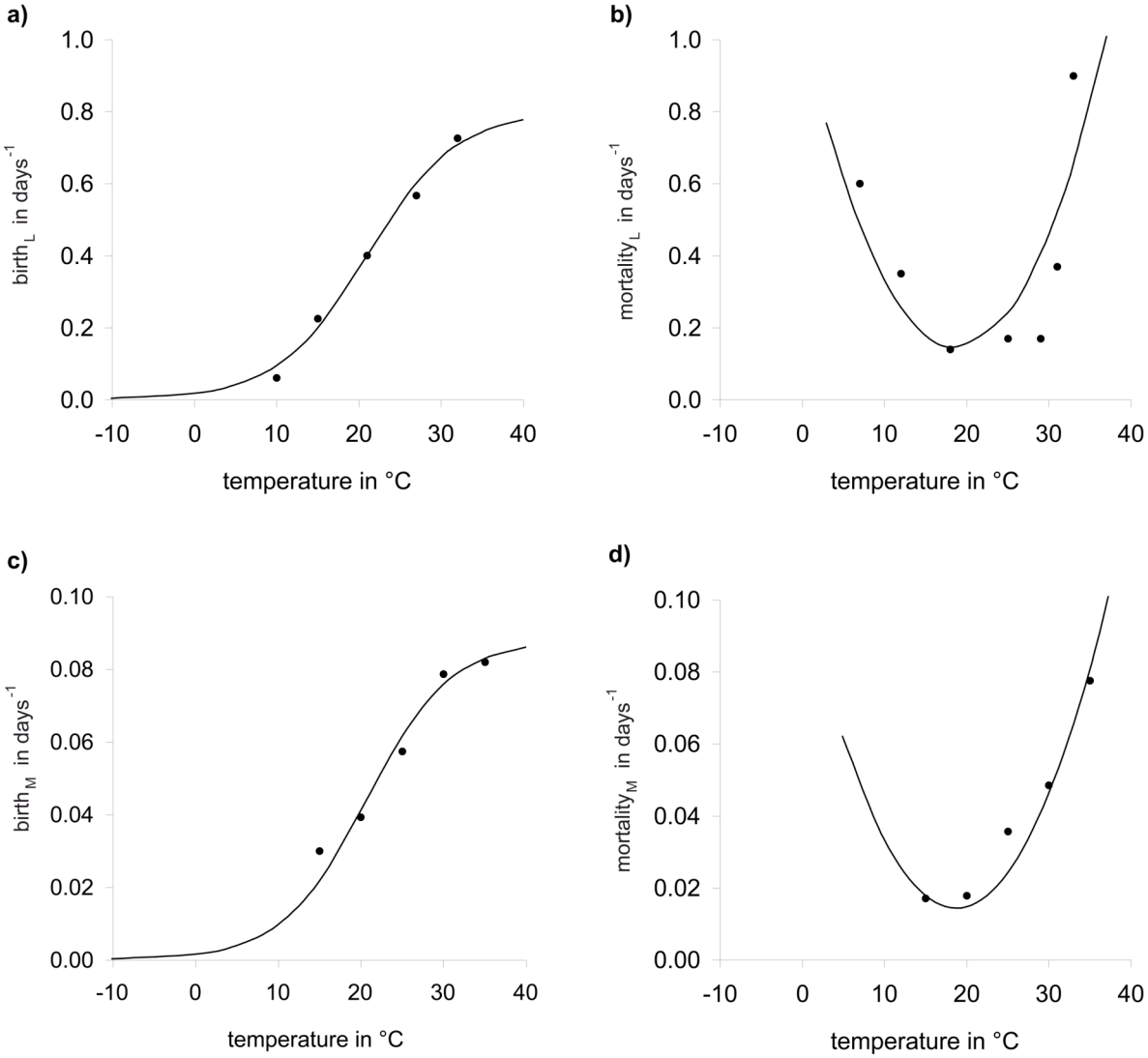

Figure 4: Observed mosquito birth and mortality rates as function of temperature. a) Function $birth_L$ fitted to data from Reisen et al. (2006) and adjusted after Rubel et al. (2008). b) Function $mortality_L$ fitted to data from Bailey and Gieke (1968). c) Function $birth_M$ fitted to data from Reisen (1995). d) Function $mortality_M$ fitted to data from Reisen (1995). Note, that the parameter functions have been selected to yield parameters for larvae that are exact one order of magnitude higher than for adult mosquitoes.

(1995) is depicted in Figure 4c. Finally, Figure 4d shows the mortality rate $mortality_M$, again as fitted to observations from Reisen (1995).

From inspection of Figure 4, it became clear that that the functions for the population parameters of the mosquito larvae are of similar shape, but about one order of magnitude higher than those for the adult mosquitoes. Using this allowed us to generalize the mosquito birth rates by using the same logistic (S-shaped) function for both, larvae and adult mosquitoes. Again, only one U-shaped function was selected to describe both mortality rates (Figures 4b and 4d), which differ by a factor of ten.

3.4 Temperature-dependent extrinsic-incubation period

The extrinsic-incubation period (*i.e.* the time from an infectious blood meal until the mosquito can transmit an acquired arbovirus infection) is an important parameter determining the vector capacity. It is the reciprocal of the rate of virus replication within an infected mosquito vector, here called infectivity rate. The parameter $infectivity_M$ is highly temperature-dependent (Cornel *et al.*, 1993; Dohm *et al.*, 2002; Turell *et al.*, 2002; Reisen *et al.*, 2006).

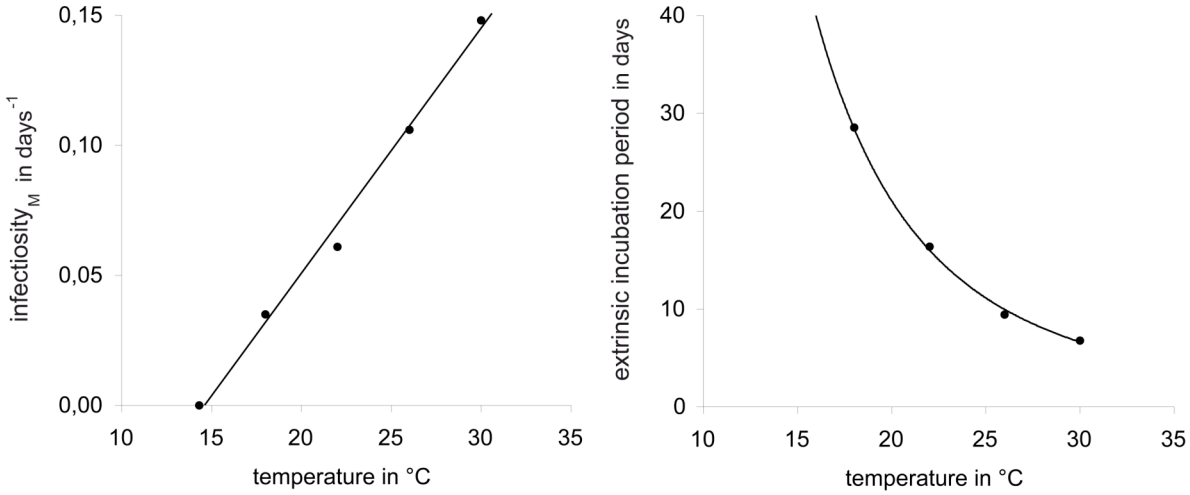

Figure 5: Observed infectivity rates (dots) and fitted function for $infectivity_M$ (left) and its reciprocal, the extrinsic-incubation period (right). Both are functions of the environmental temperature and fitted to data by Reisen et al., (2006).

Because the virus-replication rate for USUV is unknown, we relied on the results from WNV. We used data from Reisen *et al.* (2006) to fit the functions depicted in Figure 5. Thus, the extrinsic-incubation period decreases with increasing temperature. Long periods of warm temperatures amplify flavivirus transmission. Vice versa, low temperatures can reduce the flavivirus transmission or even interrupt it when the extrinsic-incubation period exceeds the mosquito lifetime.

3.5 Diapause (hibernation of mosquitoes)

Only non-diapausing mosquitoes contribute to the reproduction and the USUV transmission cycle. Therefore, it is of fundamental importance to know the fraction of non-diapausing

mosquitoes. Quantitative investigations on the diapause of *Culex* mosquitoes are rare because they had not played an important role as vector until the 1999 WNV outbreak in New York (USA). One study was published by Eldridge (1968), who depicted the proportion of non-diapausing mosquitoes as a function of photoperiod (daytime length) and temperature (Vinogradova, 2000). A second paper was presented by Spielman (2001), who re-analyzed 50-year-old-mosquito data from Boston (300 km north of the WNV outbreak in New York) to deduce a relationship between diapause and photoperiod (dots in Figure 6, left).

We fitted functions to both data sets: A 2-dimensional function (not shown) to the data of Eldridge (1968) and a 1-dimensional function to the data of Spielman (2001). Simulations demonstrated that their application yielded similar model results. This is not astonishing because of the natural correlation between the annual temperature cycle and the photoperiod. We applied the simpler relationship after Spielman (2001). The logistic function for the description of the fraction of active mosquitoes, *i.e.* the non-diapausing mosquitoes, is depicted in Figure 6 (left). It depends on the daytime length in hours, which is calculated from the astronomic declination (a function of the calendar day) and the geographic latitude. The annual cycle of the daytime lengths in Vienna is depicted in Figure 6 (right).

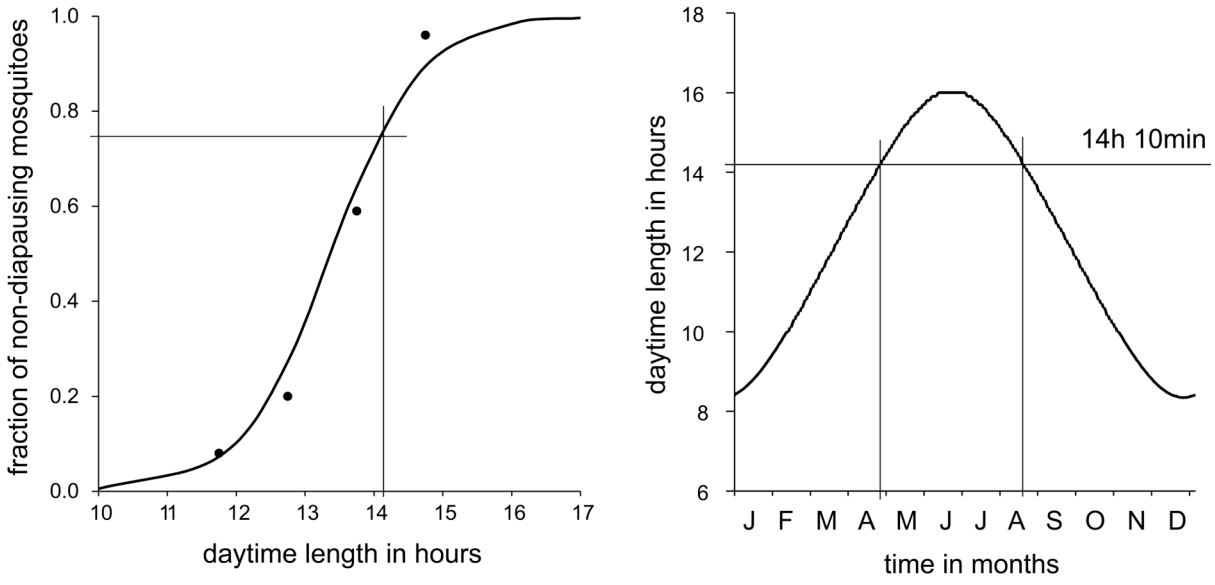

Figure 6: Observed fraction of diapausing Culex pipiens mosquitoes as function of the daytime length after Spielman (2001) with fitted function (left) and annual cycle of the daytime length in hours for the geographical latitude of Vienna, Austria (right). At daytime lengths above 14 hours and 10 minutes (May to August) more than 75 % of the mosquitoes are active.

4. Climate forcing of the observational period 2001-2005

As discussed above, the epidemic model is forced by temperature data, which determine the transmission rates $infection_B$ and $infection_M$ via the mosquito biting rate k as well as the mosquito parameters $birth_L$, $mortality_L$, $birth_M$, $mortality_M$ and $infectivity_M$.

The air-temperature measurements from the automatic weather station located at the

University of Veterinary Medicine, Vienna, were used. These measurements are available for the period 1997 to present and are representative for the study area around Vienna. The temporal resolution of the measurements is 10 minutes, providing the opportunity to run the epidemic model with time steps corresponding to this resolution.

On the other hand, the numbers of dead birds collected during the USUV monitoring program (Chvala *et al.*, 2007) are only representative on a weekly or (better) monthly time scale. Our goal was to reproduce and explain the observed multi-seasonal dynamics of USUV infections. Therefore, to account for the resolution of the observations, the model was forced by monthly averaged temperature data. Nevertheless, to assure numerical stability, the model must run with time steps of 1 day or less. We used spline functions to interpolate the monthly data to the model time step. In fact, smoothed data were used to force the model. Figure 7 (upper panel) depicts the time series of the temperature observations in Vienna for the study period 2001-2005, whereas the grey line represents the daily and the dark line the monthly averaged (smoothed) temperature. Figure 7 (lower panel) points out the temperature anomaly: the deviation from the 10-year mean 1997-2006. Conspicuously positive temperature deviations during the mosquito-activity period were observed for May to July 2002 and for May to September 2003, whereas no longer periods of extraordinary high temperatures were observed during the other years. Subject to the temperature dependence of mosquito parameters discussed in the previous section, high USUV activities were expected for 2002 and 2003. Most interesting is the year 2003, where the June to August temperatures exceed the long-term mean by more than 3 °C.

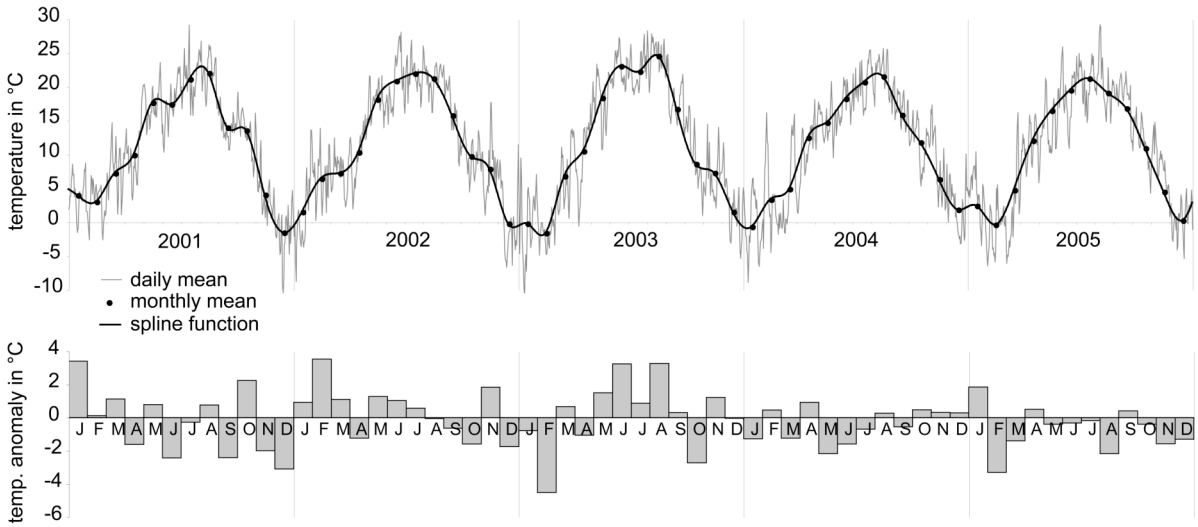

Figure 7: Observed daily and monthly averaged temperatures (upper panel) and monthly temperature anomalies (lower panel) in degree Celsius. Location Vienna, period 2001-2005. Note the positive anomalies in spring and summer 2003.

5. Short-term simulation results for the period 2001-2005

The first results of the model simulations were time series of health states of birds and mosquitoes. Figure 8 (upper panel) depicts the normalized numbers of mosquito larvae and adult mosquitoes for the investigation period 2001-2005. While the mosquito population

during the years 2001, 2004 and 2005 seemed typical, it was 2-3 times higher in 2002 and 2003. The latter were caused by the long warm periods in these years (Figure 7). The normalized number of infectious mosquitoes, I_M (Figure 8, lower panel) was influenced by the extrinsic-incubation period - which decreases with increasing temperature (Figure 5).

Figure 9 (upper panel) depicts the proportion of birds in the health states susceptible S_B, immune R_B, as well as the total population N_B. A strong increase of the immune birds $R_B = 0.7$ (70%) was simulated for 2003 in correspondence to the epidemic peak in the same year. Subsequently, R_B decreases to 45% until the end of 2004 and to 30% until the end of 2005. Analogous to the illustration of the time series of mosquitoes, Figure 9 (lower panel) depicts the proportion of infectious birds with the same epidemic peak in 2003.

For a verification of simulations with observations (Figure 10), the normalized model results were scaled to fit the observations. This has been done by multiplying the model output, *i.e.* the proportion of birds in the various health states (Figure 9), by a factor of 385 birds. This factor is the carrying capacity of birds $K_{B,obs} = 385$, which is called *observed*, because it follows from the number of observed dead blackbirds. After this scaling, our model described the observations quite well. Note that the dead-bird monitoring was organized only for the summer months June to August, while the model simulates continuously in time. Feasible comparisons may therefore only be done for the three summer months. Nevertheless, the model simulations indicate that blackbirds die from USUV during the whole mosquito activity period May to October. Based on the estimated blackbird density of 50 birds/km^2 (see

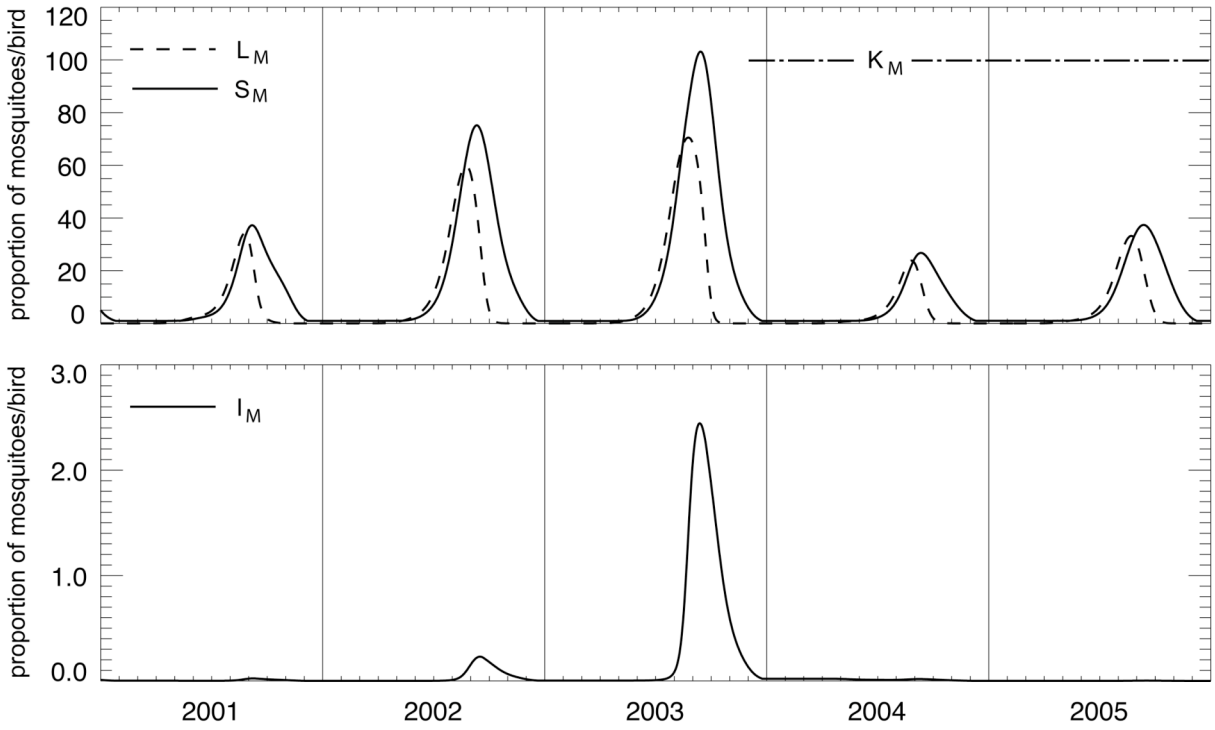

Figure 8: Simulated time series of mosquitoes for the period 2001-2005 (proportion of mosquitoes/bird). Upper panel: Larvae L_M (dotted line) and susceptible mosquitoes S_M (solid line) for carrying capacity K_M = 100 mosquito larvae/bird. Lower panel: Infectious mosquitoes I_M.

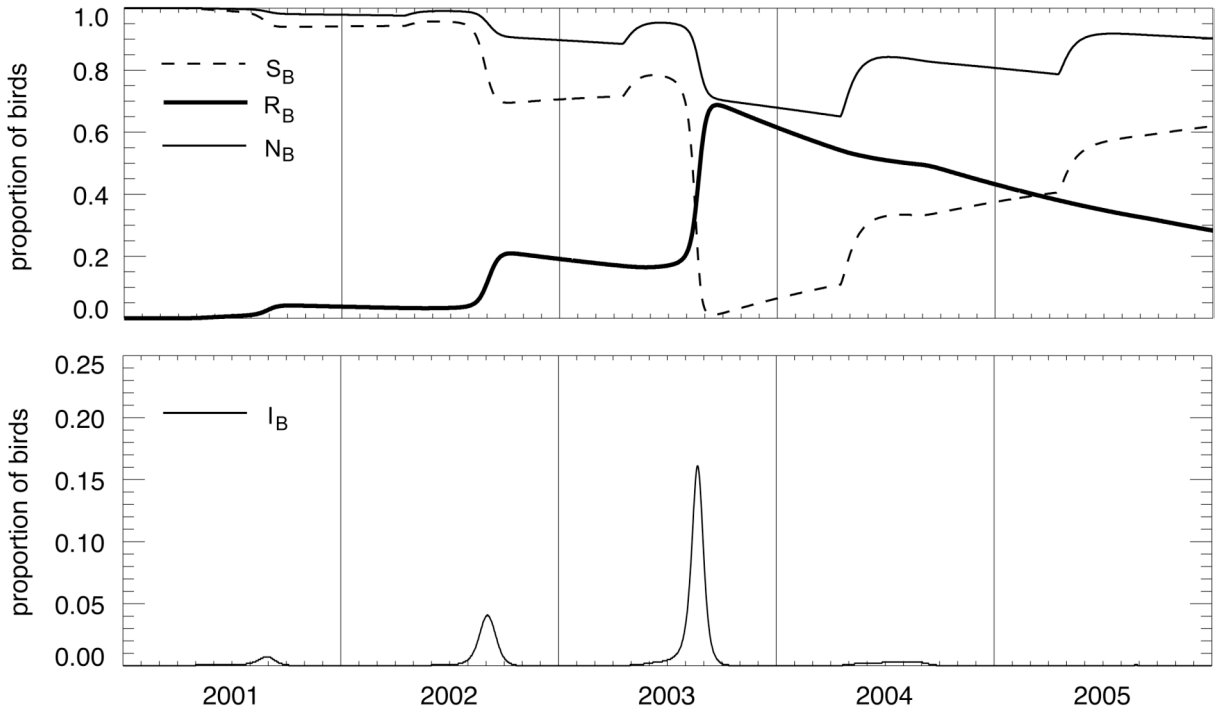

Figure 9: Simulated time series of blackbirds for the period 2001-2005 (proportion of birds related to K_B). Upper panel: Susceptible birds S_B (dotted line), immune birds R_B (bold solid line) and total birds N_B (thin solid line) for K_B = 1. Lower panel: Infectious birds I_B.

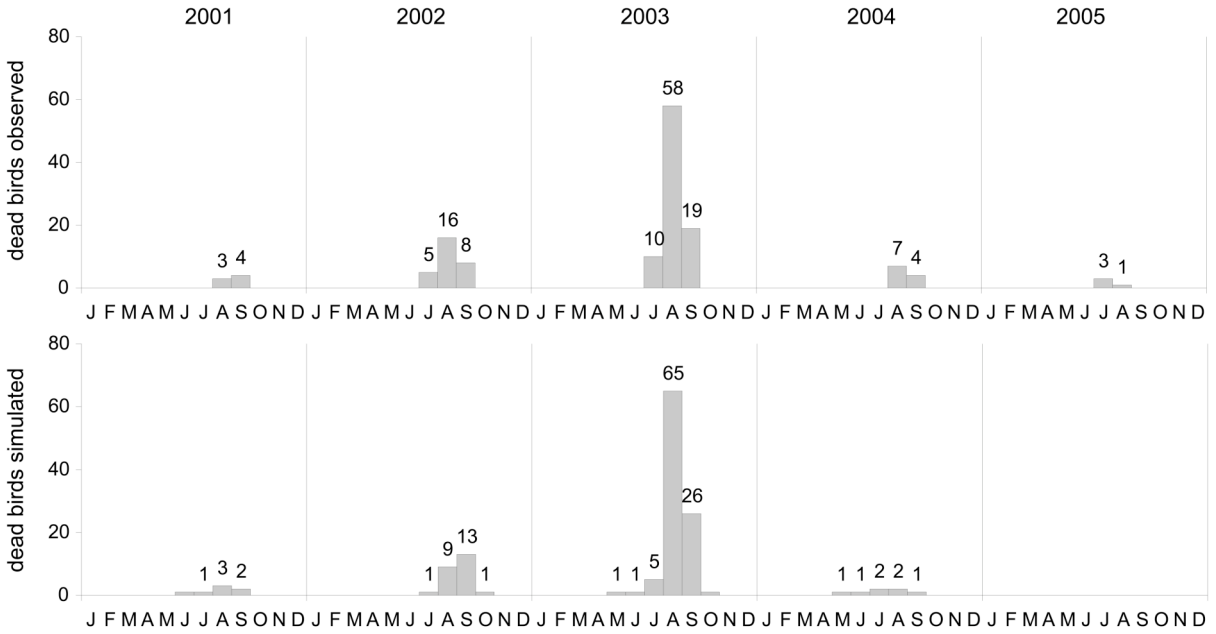

Figure 10: Time series of monthly averaged dead blackbirds for the period 2001-2005. Upper panel: Observed; lower panel: Simulated by the epidemic model (scaled with $K_{B,obs}$ = 385). Note that the number of dead birds modelled for 2005 is below 1, but non-zero.

Section 3.1) and an investigation area around Vienna of about 3,500 km^2, the true carrying capacity of blackbirds is about $K_{B,true}$ = 175,000 birds. From the fraction $K_{B,obs}/K_{B,true}$ it

follows that only 0.2% of the USUV positive birds were detected by the dead-bird monitoring program.

6. Climate forcing for the extended period 1901-2100

To simulate future USUV outbreaks, we selected the Tyndall Centre for Climate Change Research dataset, TYN SC 2.0 (Mitchell and Jones, 2005). It is based on 4 scenarios defined by IPCC and described in the Special Report on Emission Scenarios (SRES). This dataset provides the 5 climate parameters temperature, diurnal temperature range, precipitation, water-vapour pressure, and cloud cover - but we only used the temperature data. Information is presented on a 0.5° grid, equidistant in geographical latitude and longitude that covers the world land surface and is available with a monthly time-step for the period 2001-2100. Thus, the TYN SC 2.0 dataset comprises a total of 20 climate-change model runs, combining 4 possible future worlds using SRES scenarios with 5 state-of-the-art climate models (Mitchell *et al.*, 2004).

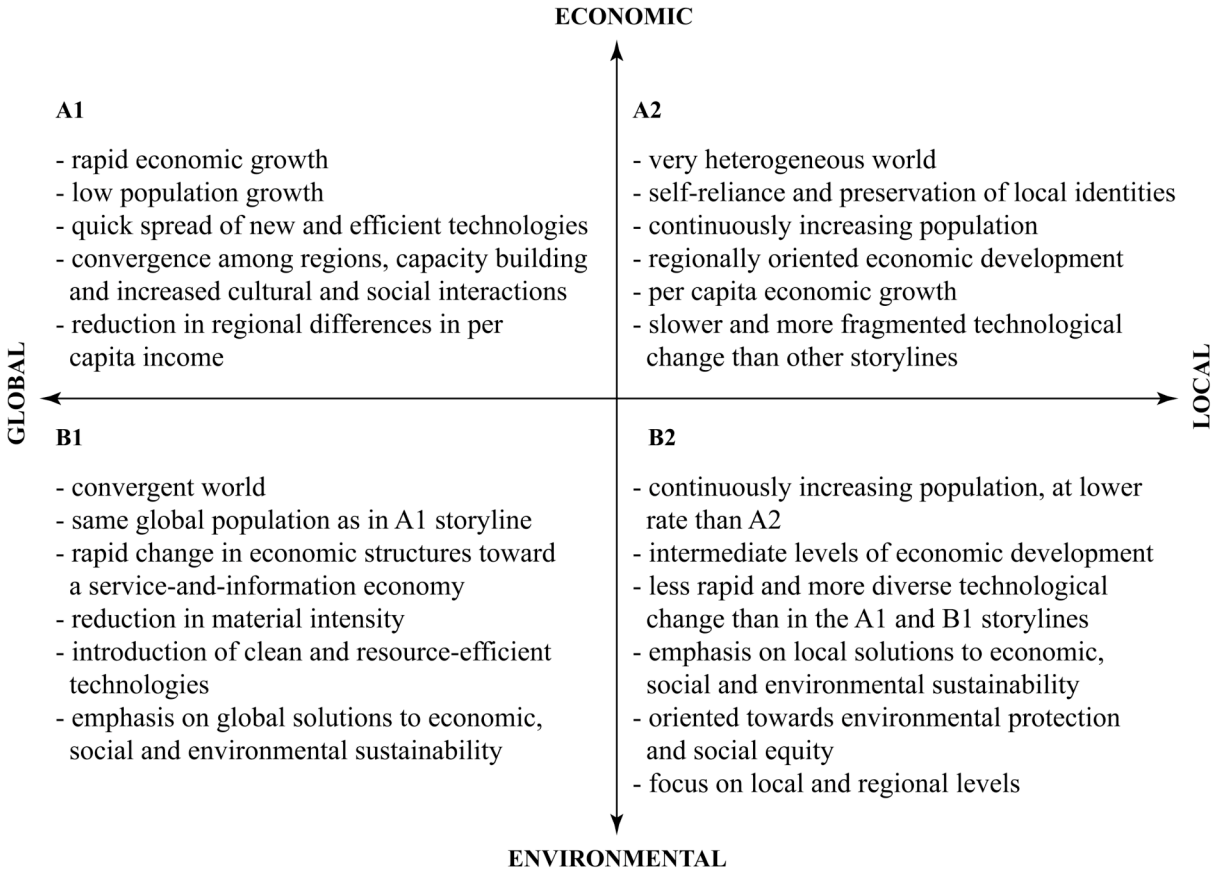

Figure 11: Brief characterization of the main Special Report on Emission Scenarios (SRES) storylines after IPCC (2000) and Arnell et al. (2004).

The emission scenarios (Figure 11) were developed in the mid 1990s and are based on 4 different narrative storylines to describe consistently the relationships between the forces driving emissions and their evolution and to add context for the scenario quantification (IPCC, 2000). The four SRES storylines represent different world futures in two dimensions: A focus on economic or environmental concerns, and global or regional development. The

variables in each model include population growth, economic development, energy use, efficiency of energy use, and mix of energy technologies, respectively. The TYN SC 2.0 dataset considers the scenarios A1 (exactly A1FI), A2, B1 and B2. On the other hand, five general circulation models were used to simulate climatic changes: The Hadley Centre Coupled Model Version 3 (HadCM3), the National Center for Atmospheric Research-Parallel Climate Model (NCAR-PCM), the Second Generation Coupled Global Climate Model (CGCM2), the Industrial Research Organization - Climate Model Version 2 (CSIRO2) and the European Centre Model Hamburg Version 4 (ECHam4).

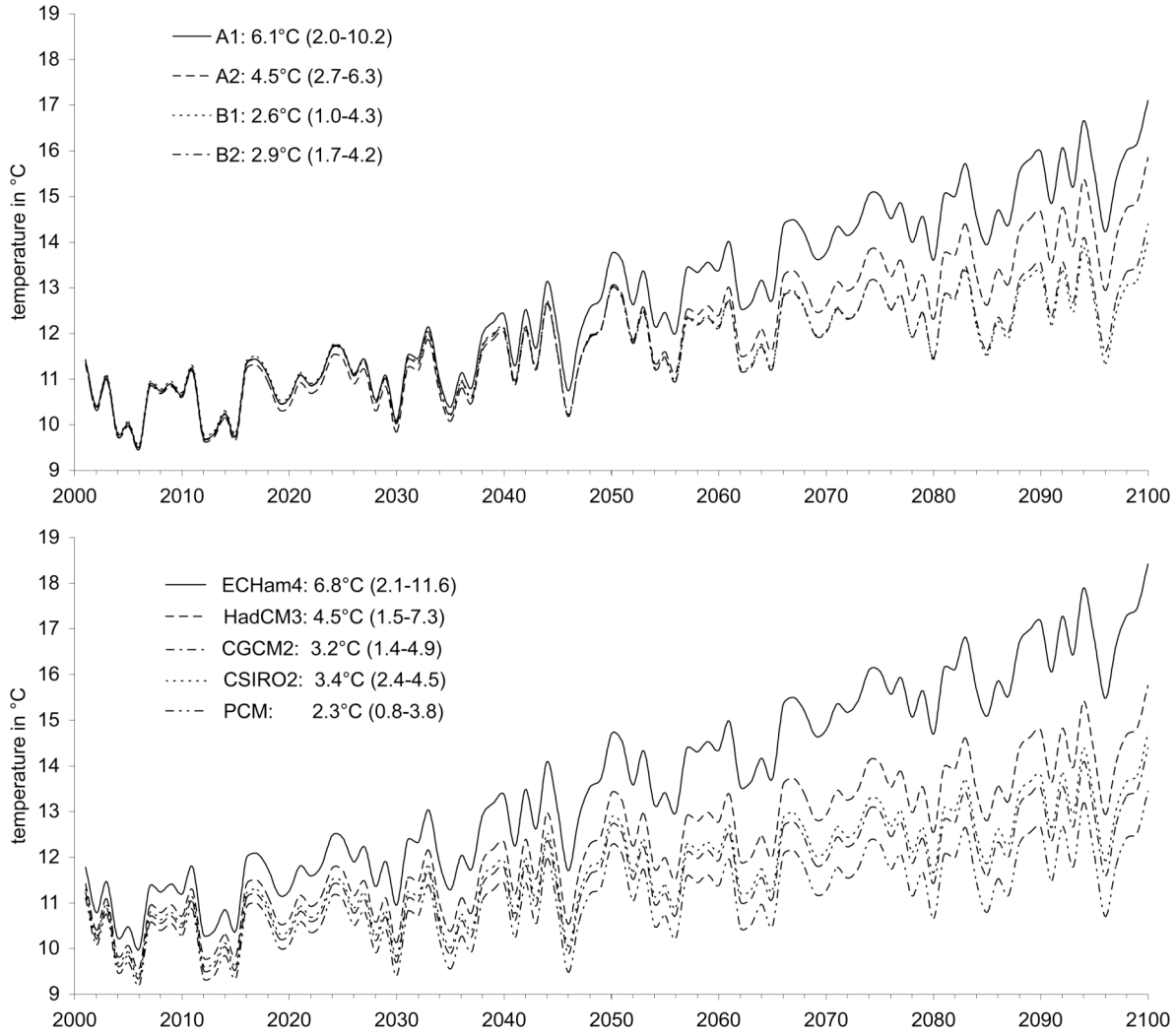

Figure 12: Time series of average annual temperature predictions for different emission scenarios (upper panel) and climate models (lower panel). Numbers in brackets denote the temperature range predicted by different climate models (upper panel) and different emission scenarios (lower panel). Grid-point Vienna, period 2001-2100.

We used only time series of monthly temperatures of the grid-point 392/277 of the TYN SC 2.0 dataset (the so-called *grid-point Vienna*), which is representative for the geographical region between 16.0-16.5° longitude and 48.0-48.5° latitude. Figure 12 depicts time series of the average annual temperature for the grid-point Vienna, grouped by scenarios (upper panel) and climate models (lower panel). All predicted temperatures show a clear trend toward

warming. The average predicted increase of the temperature during the 100-year period, calculated from the linear trend, ranged from 2.6-6.1 °C (across emission scenarios) and from 2.3-6.8 °C (across climate models). For the 20 model-scenario combinations, the range in average annual predicted warming across the century was 0.8 °C (PCM model with B1 scenario) to 11.6 °C (ECHam4 model with A1 scenario). The lowest temperature increase of 2.3 °C (0.8-3.8 °C) is simulated by the B1 scenario. It represents an environmentally oriented world with emphasis on global solutions to economic, social and environmental sustainability.

Two specific features of climate model predictions have to be considered when using it to study the evolution of biological systems (e.g. epidemic outbreaks). Firstly, climate predictions for the next 100 years merely simulate a possible temperature based on a scenario which is also a prediction. Uncertainties of these climate predictions are made evident by the range of prediction, depending on the scenario and model used. Secondly, climate models are representative for a specific spatial resolution, here of 0.5° equidistant in geographical latitude and longitude. Thus, the temperature at grid point Vienna is representative for an area of about 70 x 50 km^2 with a mean height above sea level of 261 m. The grid-point Vienna comprises, for example, the foothills of the Alps, the Vienna Forest, and planes like the Tullner Feld (*i.e.* the resolution is too coarse for our study area). USUV cases have been observed only in the flat country where temperatures are high. These temperatures were measured by our weather station located at 153 m above sea level. Therefore, the temperatures simulated by climate models were adjusted to the measured temperatures (downscaled) to describe this small-scale region (Rubel *et al.*, 2008). Note that it is essential to use the (generally slightly higher) downscaled temperature predictions to force the USUV model. Otherwise the effect of the climate warming signal would be compensated by the underestimation of the temperatures predicted by the large-scale climate models.

7. Long-term simulation results for the period 1901-2100

The time series of predicted annually averaged numbers of birds dead because of USUV is depicted in Figure 13. The upper panel shows the mean proportion of dead birds together with the 95% confidence interval (grey areas) calculated from 5 model runs forced by the GCM predictions for the worst-case emission scenario A1. The lower panel shows the same for the best-case scenario B1.

The main result is that USUV was predicted to survive in almost all model simulations except those simulations where the USUV model is driven by temperatures from PCM using the A1 and A2 scenarios. This virus extinction leads to the higher variation of the proportion of dead birds in the A1 scenario. After the epidemic peak 2003, only minor outbreaks are simulated until the next major outbreak in 2019. The amplitude of the outbreaks, here the annually accumulated proportions of dead blackbirds, vary accordingly to the predicted temperatures. The higher temperature increase of the A1 scenario results in the higher predicted annual USUV specific mortality risk in the blackbirds. Moreover, forcing the USUV model with temperatures from two climate models (ECHam4 and HadCM3 with A1 scenario) result in an endemic situation with a constant level of about 11% dead birds in the year 2050. Typically, a cyclic annual mortality pattern was predicted through the years – but the predicted amplitude of the cycle of annual mortality decreases later in the century especially of the A1 emission scenario. For the A1 scenario on average 60% of all birds acquire immunity until the end of the century. But also for the best-case scenario B1, a proportion of 50% of the birds acquire lifelong immunity.

Additionally, we depict the USUV dynamics by the annual basic reproduction number R_0 as derived and discussed by Rubel *et al.* (2008). Figure 14 shows the time series of R_0 for the period 1901-2100. While IPCC scenarios have been used to predict the future, observed temperature values were taken to calculate a projection to the past. Major outbreaks may only occur for $R_0 > 1$, firstly calculated for the observed USUV epidemics 2001-2005. Thus, our backward projection using observed temperatures shows that USUV was not able to cause major outbreaks in the past. Nevertheless, minor outbreaks below some detection threshold were possible, because of the annual cycle of R_0 (not shown).

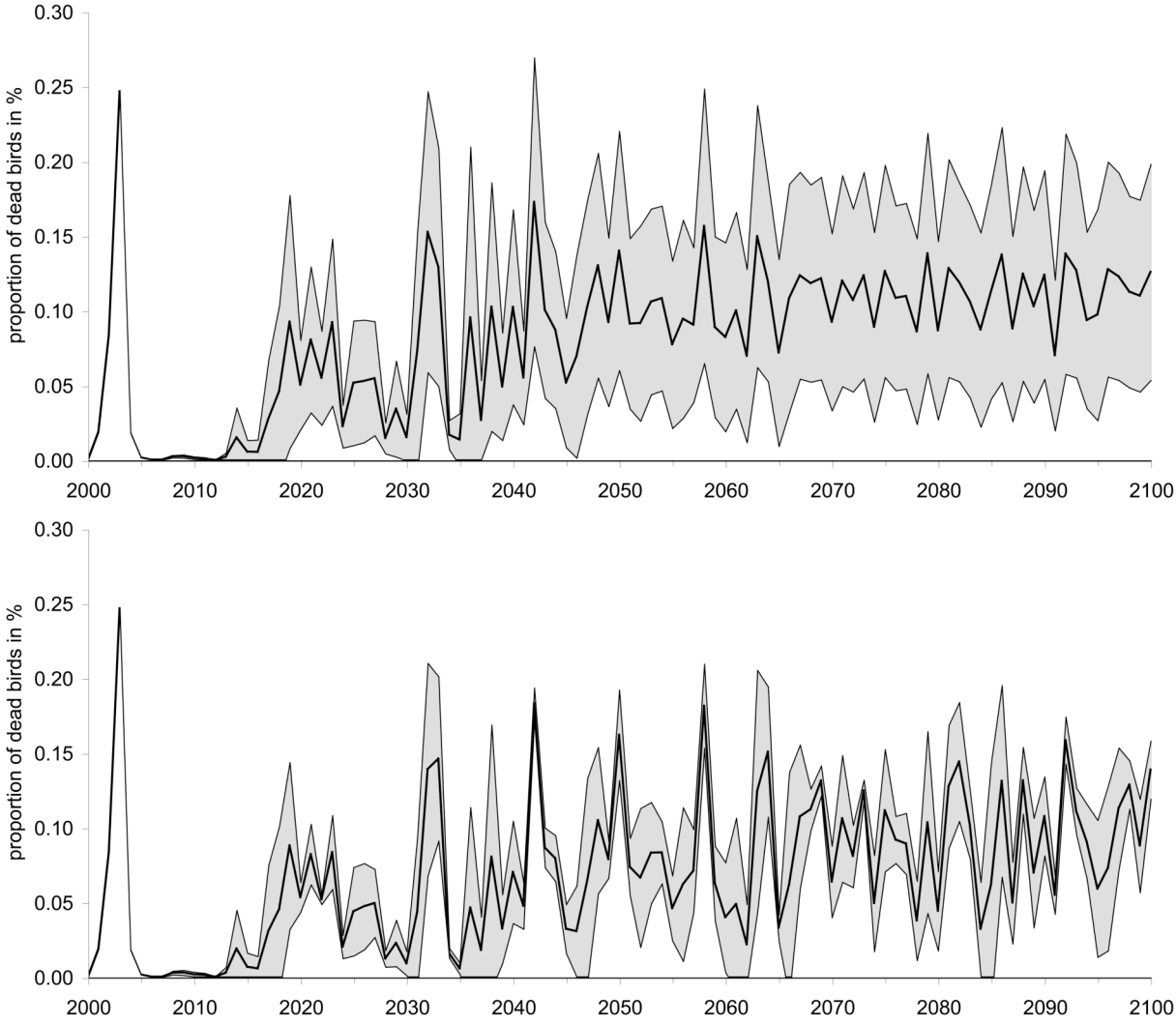

Figure 13: Average (central line) and 95 % confidence interval (grey areas) of USUV-specific mortality of blackbirds around Vienna. Emission scenario A1 (upper panel) and B1 (lower panel).

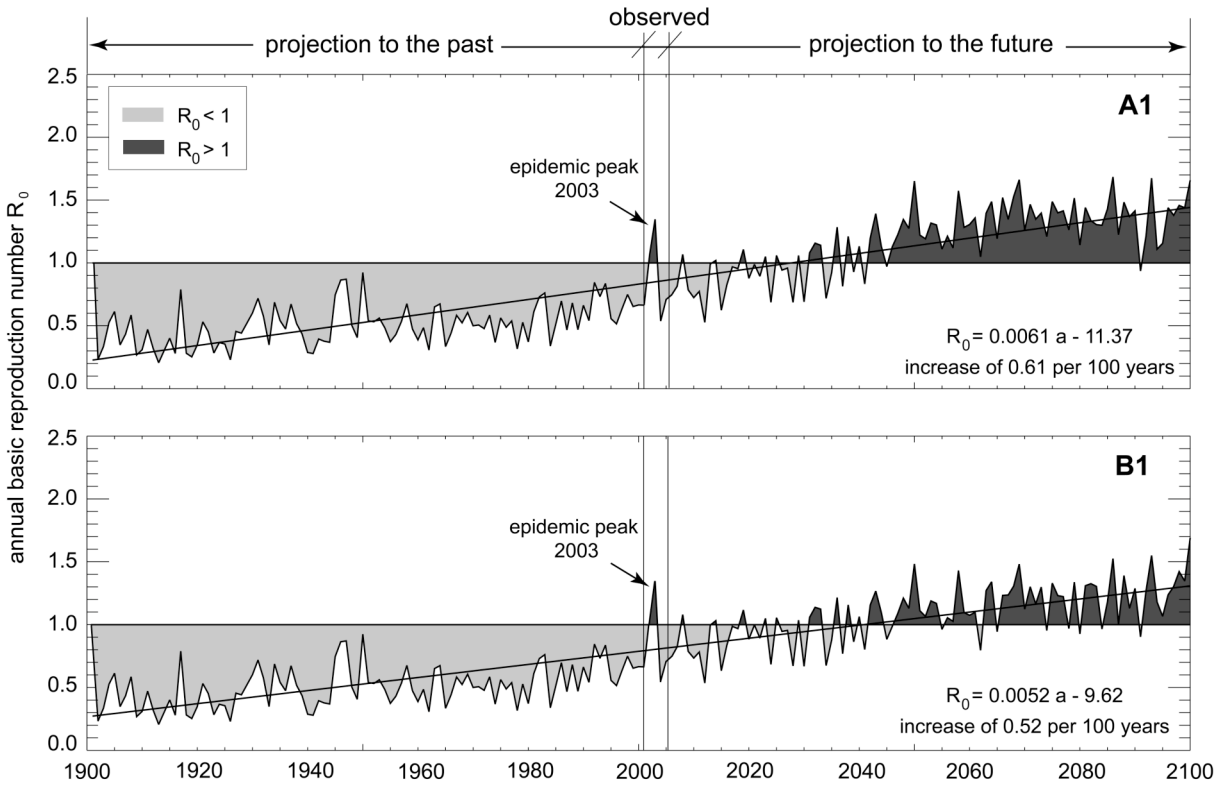

Figure 14: Mean annual basic reproduction numbers for the IPCC worst-case scenarios A1 (upper panel) and best-case scenarios B1 (lower panel). Linear trends for the period 1901-2100 indicate an increase of R_0 = 0.61 per 100 years for the A1 and R_0 = 0.52 per 100 years for the B1 scenario.

8. Discussion

What has been achieved?

As an example for viral zoonoses affecting wildlife and domestic animals, the dynamics of the well-documented USUV epidemics in Vienna was investigated. After the epidemic peak, more than 70% of the bird population acquired immunity. However, the immunity decreases very quickly and already some years after the epidemic peak in 2003 a new major outbreak can occur, depending only on the environmental temperature. Other environmental parameters such as precipitation or flooding seem to play only a minor role (because our model fitted well without them). The 100-year flood in Vienna in August 2002, for example, had no effect on the USUV epidemics. Similar observations were made in the U.S. in connection with the hurricane Katrina and WNV (Farnon, 2006). The so-called floodwater mosquitoes are minor effective vectors for WNV and USUV.

From 20 scenario-model combinations we examined, only two were predicted to lead to extinction of USUV (PCM, A1 and A2 scenarios). The other 18 combinations lead to endemicity in Central Europe through the end of the century. It is therefore very likely, that the virus survives in Central Europe until the end of the century. We do not further investigate the possibilities for local extinction because we assume that the USUV is continuously introduced by migratory birds. Thus, the most important epidemiological quantity determining major outbreaks is the basic reproduction number R_0. It predicts optimal environmental conditions for USUV outbreaks due to global warming in about 10 years. On

the other hand, undetected USUV outbreaks before the observed outbreak in 2003 are very unlikely.

Our model explains the USUV transmission by combining both the effect of the immunity status of the bird population and effects of the environmental temperature. Additionally, the parameter estimation was confirmed by the results of a Bayes analysis (Reiczigel *et al.*, 2010). Thus, we propose the application of the model presented here for studies on WNV transmission in North America.

What has been neglected?

Our estimations seem realistic when compared to the observed large-scale declines in the bird populations caused by WNV infections in North America (LaDeau *et al.*, 2007). Possible effects of global warming concerning bird and mosquito populations due to changes in land cover, availability of food or other environmental factors have not been considered; *i.e.*, the carrying capacity of birds K_B and mosquitoes K_M were assumed to be constant during the investigation period 2001-2100. Further, we did not consider either vertical transmission of USUV in the mosquito vectors or horizontal transmission in susceptible birds. This decision was made because there exist no data at all on these particular transmission scenarios in USUV infections. In addition, these modes of transmission have been experimentally shown in infections with the related WNV, but their relevance in field infections seems negligible (Baqar *et al.*, 1993; Komar *et al.*, 2003).

What needs to be done?

A comprehensive verification of the arbovirus model might be realized in a few years when longer time series of observations are available. Especially, the population dynamics of mosquitoes of the *Culex pipiens* complex have to be verified. Unfortunately, there are no current entomological field studies in Austria. Also, the assumption that the extrinsic incubation period of USUV (which has never been investigated in laboratory experiments) is similar to that of the closely related WNV has to be verified. Other recently published verification datasets comprise the abundance of blackbirds. Steiner and Holzer (2008), for example, investigated the decline of blackbirds at 6 locations in Vienna. They found big local differences in time and extent of mass mortality in blackbirds. While the decline in bird populations was about 58% in some regions near the Danube River, in other regions more than 94% of blackbirds disappeared. This disagrees with the experience of G. Loupal (personal communications), who stated that the blackbird population was not dramatically influenced by the USUV epidemics, as it has also been confirmed by observations.

Acknowledgements

The authors are very grateful to Prof. Dr. Herbert Weissenböck and Dr. Sonja Chvala-Mannsberger, both University of Veterinary Medicine Vienna, for their dead-bird surveillance data and to Dr. Ingeborg Auer from the Austrian weather service (*Zentralanstalt für Meteorologie und Geodynamik*, ZAMG) for kindly providing the map of hot days as well as the time series of observed temperature data. The Tyndall Centre for Climatic Change Research at the University of East Anglia, UK, provided the GCM projections.

References

Arnell, N.W., Livermore, M.J.L., Kovats, S., Levy, P.E., Nicholls, R., Parry, M.L. and Gaffin, S.R., 2004. Climate and socio-economic scenarios for global-scale climate change impacts assessments: Characterising the SRES storylines. Global Environ. Chang. 14, 3-20.

Auer, I., Böhm, R., Mohni, H., Potzmann, R., Schöner, W. and Skomorowski, P., 2001. ÖKLIM - the digital Climate Atlas of Austria - an interactive trip through the past, present and future climate (in German). CD-ROM, Zentralanstalt für Meteorologie und Geodynamik.

Bailey, S.F. and Gieke, P.A., 1968. A study of the effect of water temperature on rice field mosquito development. Proc. Calif. Mosq. Vector Control Assoc. 36, 53-61.

Bakonyi, T., Erdélyi, K., Ursu, K., Ferenczi, E., Csörgö, T., Lussy, H., Chvala, S., Bukovsky, C., Meister, T., Weissenböck, H. and Nowotny, N., 2007. Emergence of Usutu virus in Hungary. J. Clin. Microbiol. 45, 3870-3874.

Baqar, S., Hayes, C.G., Murphy, J.R. and Watts, D.M., 1993. Vertical transmission of West Nile virus by *Culex* and *Aedes* species mosquitoes. Am. J. Trop. Med. Hyg. 48, 757-762.

Brugger, K. and Rubel, F., 2009. Simulation of climate-change scenarios to explain Usutu-virus dynamics in Austria. Prev. Vet. Med. 88, 24-31.

Cavrini, F. and Co-authors, 2009. Usutu virus in a patient who underwent orthotrophic liver transplantation, Italy, August-September 2009. Euro Surveill. 14(50), 1-2.

Chvala, S., Bakonyi, T., Bukovsky, C., Meister, T., Brugger, K., Rubel, F., Nowotny, N. and Weissenböck, H., 2007. Monitoring of Usutu virus activity and spread by using dead bird surveillance in Austria, 2003-2005. Vet. Microbiol. 122, 237-245.

Cornel, A.J., Jupp, P.G. and Blackburne, N.K., 1993. Environmental-temperature on the vector compedence of *Culex univittatus* (Diptera, Culiciade) for West Nile virus. J. Med. Entomol. 30, 449-456.

Cruz-Pacheco, G., Esteva, L., Montaño-Hirose, J.A. and Vargas, C., 2005. Modelling the dynamics of West Nile Virus. Bull. Math. Biol. 67, 1157-1172.

Dohm, D.J., O'Guinn, M.L. and Turell, M.J., 2002. Effect of environmental temperature on the ability of *Culex pipiens* (Diptera: Culicidae) to transmit West Nile virus. J. Med. Entomol. 39, 221-225.

Eisenberg, J.N., Reisen, W.K. and Spear, R.C., 1995. Dynamic model comparing the bionomics of two isolated *Culex tarsalis* (Diptera: Culicidae) populations: Model development. J. Med. Entomol. 32, 83-97.

Eldridge, B.F., 1968. The effect of temperature and photoperiod on blood-feeding and ovarian developmentin mosquitoes of *Culex pipiens* complex. Am. J. Trop. Med. Hyg. 17, 133-140.

Farnon, E.C., 2006. Summary of West Nile virus activity, United States 2005. 7th Nat. Conf. on West Nile Virus in the U.S., San Francisco, California, Feb. 23-24. Available at: http://www.cdc.gov/ncidod/dvbid/westnile/conf/February 2006.htm.

Gale, P., Brouwer, A., Ramnial, V., Kelly, L., Kosmider, R., Fooks, A.R. and Snary E.L., 2010. Assessing the impact of climate change on vector-borne viruses in the EU through the elicitation of expert opinion. Epidemiol. Infect. 138, 214-225.

Harvell, C., Mitchell, C., Ward, J., Altizer, S., Dobson, A., Ostfeld, R. and Samuel, M., 2002. Climate warming and disease risks for terrestrial and marine biota. Science 296, 2158-2162.

Hatchwell, B.J., Chamberlain, D.E. and Perris, C.M., 1996. The demography of blackbirds *Turdus merula* in rural habitats: Is farmland a sub-optimal habitat? J. Appl. Ecol. 33, 1114-1124.

IPCC (Intergovernmental Panel on Climate Change), 2000. Intergovernmental Panel on Climate Change Special Report on Emissions Scenarios. Cambridge University Press, UK, pp. 570. Available at: http://www.grida.no/climate/ipcc/emission/.

Komar, N., Langevin, S., Hinten, S., Nemeth, N., Edwards, E., Hettler, D., Davis, B., Bowen, R. and Bunning, M., 2003. Experimental infection of North American birds with the New York 1999 strain of West Nile virus. Emerg. Infect. Dis. 9, 311-322.

LaDeau, S.L., Kilpatrick, A.M. and Marra, P.P., 2007. West Nile virus emergence and large-scale declines of North American bird populations. Nature 447, 710-713.

Lelli, R., Savini, G., Teodori, L., Filipponi, G., Gennaro, A.D., Leone, A., Gialleonardo, L. D.,

Venturi, L. and Caporale, V., 2008. Serological evidence of Usutu virus occurrence in north-eastern Italy. Zoon. Publ. Health 55, 361-367.

Manarolla, G., Bakonyi, T., Gallazzi, D., Crosta, L., Weissenböck H., Dorrestein, G.M. and Nowotny, N., 2010. Usutu virus in wild birds in northern Italy. Vet. Microbiol. 141, 159-163.

Meister, T., Lussy, H., Bakonyi, T., Sikutová, S., Rudolf, I., Vogl, W., Winkler, H., Frey, H., Hubálek, Z., Nowotny, N. and Weissenböck, H., 2008. Serological evidence of continuing high Usutu virus (Flaviviridae) activity and establishment of herd immunity in wild birds in Austria. Vet. Microbiol. 127, 237-248.

Mitchell, T.D., Carter, T.R., Jones, P.D., Hulme, M. and New, M., 2004: A comprehensive set of high-resolution grids of monthly climate for Europe and the globe: the observed records (1901-2000) and 16 scenarios (2001-2100). Tyndall Centre of Climate Change Research, Working Paper 55. Available at: http://www.tyndall.ac.uk/content /comprehensive-set-high-resolution-grids-monthly-climate-europe-and-globe-observed-record-190.

Mitchell, T.D. and Jones, P.D., 2005. An improved method of constructing a database of monthly climate observations and associated high-resolution grids. Int. J. Climatol. 25, 693-712.

Olejnícek, J. and Gelbic, I., 2000. Differences in response to temperature and sensity between two strains of the mosquito, *Culex pipiens molestus forskal*. J. Vector Ecol. 25, 136-145.

Pecorari, M., Longo, G., Gennari, W., Grottola, A., Sabbatini, A.M., Tagliazucchi, S., Savini, G., Monaco, F., Simone, M.L., Lelli, R. and Rumpianesi, F., 2009. First human case of Usutu virus neuroinvasive infection, Italy, August-September 2009. Euro Surveill. 14(50). Available at: http://www.eurosurveillance.org/ViewArticle.aspx?ArticleId =19446.

Pfeffer, M. and Dobler, G., 2009. Was kommt nach Bluetongue – Europa im Fadenkreuz exotischer Viren (in German). Berl. Münch. Tierärztl. Wochenschr. 122, 458-466.

Pfeffer, M. and Dobler, G., 2010. Emergence of zoonotic arboviruses by animal trade and migration. Parasites & Vectors 3:35, doi:10.1186/1756-3305-3-35.

Rae, D.J., 1990. Survival and development of the immature stages of *Culex annulirostris* (Diptera: Culicidae) at the Ross River Dam in tropical eastern Australia. J. Med. Entomol. 27, 756-762.

Reiczigel, J., Brugger, K., Rubel, F., Solymosi, N. and Lang, Z., 2010. Bayesian analysis of a dynamical model for the spread of the Usutu virus. Stoch. Environ. Res. Risk Assess. 24, 455-462.

Reisen, W.K., 1995. Effect of temperature on *Culex tarsalis* (Diptera: Culicidae) from the Coachella and San Joaquin valleys of California. J. Med. Entomol. 32, 636-645.

Reisen, W.K., Fang, Y. and Martinez, V.M., 2006. Effects of temperature on the transmission of West Nile virus by *Culex tarsalis* (Diptera: Culicidae). J. Med. Entomol. 43, 309-317.

Rubel, F., Brugger, K., Hantel, M., Chvala, S., Bakonyi, T., Weissenböck, H. and Nowotny, N., 2008. Explaining USUTU virus dynamics in Austria: Model development and calibration. Prev. Vet. Med. 85, 166-186.

Rueda, L.M., Patel, K.J., Axtell, R.C. and Stinner, R.E., 1990. Temperaturedependent development and survival rates of *Culex quinquefasciatus* and *Aedes aegypti* (Diptera: Culicidae)). J. Med. Entomol. 27, 892-898.

Schnack, S., 1991. The breeding ecology and nestling diet of Blackbird *Turdus merula* L. and Song Thrush Turdus philomelos C. L. Brehm in Vienna and adjancent wood. Acta Ornithol. 26, 85-106.

Schönwiese, C.-D., Staeger, T. and Trömel, S., 2004. The hot summer 2003 in Germany. Some preliminary results of a statistical time series analysis. Meteorol. Z. 13, 323-327.

Schwarz, J. and Flade, M., 1989. Ergebnisse des DDA-Monitoringprogramms Teil I: Bestandsänderungen von Vogelarten der Siedlungen seit 1989 (in German). Vogelwelt 121, 87-106.

Shaman, J.M., Spiegelman, M., Cane, M. and Stieglitz, M., 2006. A hydrologically driven model of swamp water mosquito population dynamics. Ecol. Mod. 194, 395-404.

Spielman, A., 2001. Structure and seasonality of nearctic *Culex pipiens* populations. Ann. NY. Acad. Sci. 951, 220-234.

Steiner, H.M. and Holzer, T., 2008. Local differences in time and extent of mass mortality in Blackbirds (*Turdus merula L.*) after emergence of Usutu virus (USUV; Flaviviridae) in Vienna, Austria (in German). Vogelwarte 46, 25-35.

Tomialojc, L., 1993. Breeding ecology of blackbird *Turdus merula* studied in the primaeval forest of Bialowieza (Poland). Part 1. Breeding numbers, distribution and nest sites. Acta Ornithol. 27, 131-157.

Tomialojc, L., 1994. Breeding ecology of blackbird *Turdus merula* studied in the primaeval forest of Bialowieza (Poland). Part 2. Reproduction and mortality. Acta Ornithol. 29, 101-121.

Turell, M.J., Sardelis, M.R., O'Guinn, M.L. and Dohm, D.J., 2002. Potential vectors for West Nile virus in North America. Curr. Top. Microbiol. Immunol. 267, 241-252.

Vinogradova, E.B., 2000. *Culex Pipiens Pipiens* Mosquitoes. Pensoft, Sofia-Moscow, pp. 250.

Weissenböck, H., Kolodziejek, J., Fragner, K., Kuhn, R., Pfeffer, M. and Nowotny, N., 2003. Usutu virus activity in Austria, 2001-2002. Microbes Infect. 5, 1132-1136.

Weissenböck, H., Kolodziejek, J., Url, A., Lussy, H., Rebel-Bauder, B. and Nowotny, N., 2002. Emergence of Usutu virus, an African mosquito-borne flavivirus of the Japanese encephalitis virus group, central Europe. Emerg. Infect. Dis. 8, 652-656.

Wichmann, G. and Zuna-Kratky, T., 1997. Monitoring von Wald- und Kulturlandschafts-Vögeln an zwei Probeflächen bei Wien-Kalksburg (in German), pp. 85. A study of Bird Life Austria. Available at: www.magwien.gv.at/umweltschutz/pool/pdf/kalksburg.pdf.

Wonham, M.J., de Camino-Beck, T. and Lewis, M.A., 2004. An empidemiological model for West Nile virus: Invasion analysis and control applications. Proc. R. Soc. Lond. B 271, 501-507.

Appendix A The USUV model

Model equations

$$\frac{dS_B}{dt} = (b_B - (b_B - m_B)\, N_B/K_B)\, N_B - \delta_M\, \beta_M(T)\, I_M\, S_B/K_B \; - \; m_B\, S_B \tag{1}$$

$$\frac{dE_B}{dt} = \delta_M\, \beta_M(T)\, I_M\, S_B/K_B - \gamma_B\, E_B \; - \; m_B\, E_B \tag{2}$$

$$\frac{dI_B}{dt} = \gamma_B\, E_B \; - \alpha_B\, I_B \; - \; m_B\, I_B \tag{3}$$

$$\frac{dR_B}{dt} = (1 - \nu_B)\, \alpha_B\, I_B \; - \; m_B\, R_B \tag{4}$$

$$\frac{dD_B}{dt} = \nu_B\, \alpha_B\, I_B \tag{5}$$

$$\frac{dL_M}{dt} = (b_L(T)\, \delta_M\, N_M - m_L(T) L_M)(1 - L_M/K_M) - b_M(T)\, L_M \tag{6}$$

$$\frac{dS_M}{dt} = -\delta_M\, \beta_B(T)\, S_M\, I_B/K_B + b_M(T)\, L_M - m_M(T)\, S_M \tag{7}$$

$$\frac{dE_M}{dt} = \delta_M\, \beta_B(T)\, S_M\, I_B/K_B - \gamma_M(T)\, E_M - m_M(T)\, E_M \tag{8}$$

$$\frac{dI_M}{dt} = \gamma_M(T)\, E_M - m_M(T)\, I_M \tag{9}$$

Health states

S_B	susceptible birds
E_B	latent-infected or exposed birds
I_B	infectious birds
R_B	recovered or immune birds
D_B	dead birds
L_M	larvae mosquitoes
S_M	susceptible mosquitoes
E_M	latent-infected or exposed mosquitoes
I_M	infectious mosquitoes

Main Parameters

$birth_B$	birth rate birds	$b_B = 0.073\,((d-105)/19.3)^{-0.52}\,exp(-(d-105)/19.3)$
$mortality_B$	mortality rate birds	$m_B = 0.0012$
$infection_B$	force of infection	$\lambda_B = 0.04175/[1 + 1.231\,exp(-0.184\,(T-20))]$
$infectivity_B$	1/intrinsic incubation period	$\gamma_B = 0.667$
$recovery_B$	recovery rate birds	$\alpha_B\,(1-\nu_B) = 0.1274$
$death_B$	death rate due infection	$\alpha_B\,\nu_B = 0.0546$
$birth_L$	birth rate larvae	$b_L = 0.7998/[1 + 1.231\,exp(-0.184\,(T-20))]$
$mortality_L$	mortality rate larvae	$m_L = 0.0025\,T^2 - 0.094\,T + 1.0257$
$birth_M$	birth rate mosquito	$b_M = b_L/10$
$mortality_M$	mortality rate mosquito	$m_M = m_L/10$
$infection_M$	force of infection	$\lambda_M = 0.344/[1 + 1.231\,exp(-0.184\,(T-20))]$
$infectivity_M$	1/extrinsic incubation period	$\gamma_M = 0.0093\,T - 0.1352 \quad (T > 15°C)$

Additional Parameters

k	biting rate of mosquitoes	$k = 0.344/[1 + 1.231\,exp(-0.184\,(T-20))]$
p_M	probability transm. M $\rightarrow$ B	$p_M = 1.0$
p_B	probability transm. B $\rightarrow$ M	$p_B = 0.125$
β_M	transmission rate M $\rightarrow$ B	$\beta_M = k\,p_M$
β_B	transmission rate B $\rightarrow$ M	$\beta_B = k\,p_B$
K_B	carrying capacity, birds	
K_M	carrying capacity, mosquitoes	
N_B	total bird population	
N_M	total mosquito population	
δ_M	non-diapausing mosquitoes	$\delta_M = 1 - 1/[1 + 1775.7\,exp(1.559(D-18.177))]$
D	daytime length	$D = 7.639\,arcsin[tan(\epsilon)\,tan(\varphi) + 0.0146/(cos(\epsilon)\,cos(\varphi))]$
ϵ	declination	$\epsilon = 0.409\,sin[2\,\pi(d-80)/365]$
d	calendar day	
φ	geographic latitude	

Appendix B R-Source-code for the USUV model

```
## R source code for USUV-model                                                    ##

quartz(height=6, width=4); par(mfrow=c(4, 1), mar=c(4, 4.5, 0.5, 0.5))

# input data: monthly temperatures for Vienna 2001-2005

T_month=c(4.0,3.0,7.2,9.9,17.7,17.4,21.1,22.0,14.0,13.6,4.0,-1.6,
    1.5,6.4,7.2,10.3,18.1,20.9,22.0,21.2,15.8,9.7,7.9,-0.2,
    -0.2,-1.6,6.8,10.5,18.4,23.1,22.3,24.5,16.7,8.6,7.3,1.5,
    -0.7,3.4,4.9,12.5,14.7,18.2,20.7,21.5,15.9,11.8,6.3,1.8,
    2.4,-0.4,4.7,12.1,16.5,19.5,21.2,19.1,16.8,10.9,4.5,0.2)
T_sp=spline(T_month,n=30*length(T_month)) # interpolation to daily values
T<-as.vector(unlist(T_sp[2]))
l=length(T)
T<-T[c((l-15):l,1:(l-14))]

n=length(T)-1
t=seq(0,n)


# parameter

k=seq(0, n); k=0.344/(1+1.231*exp(-0.184*(T-20)))
bL=seq(0, n); bL=2.325*k; bM=bL/10
mL=seq(0, n); mL=0.0025*T^2-0.094*T+1.0257; mM=mL/10
phi=48.21*pi/180
day=c(0, rep(seq(1, 365), 6))
epsilon=seq(0, n); epsilon=0.409*sin(2*pi*(day-80)/365)
D=seq(0, n); D=7.639*asin(tan(epsilon)*tan(phi)+0.0146/(cos(epsilon)*cos(phi)))+12
dM=seq(0, n); dM=1-1/(1+1775.7*exp(1.559*(D-18.177)))

KM=100
KB=1

gammaM=seq(0, 0, length=n+1)
for (i in 1:n){
  if (T[i]>15) gammaM[i]=0.0093*T[i]-0.1352
}

bB=seq(0, 0, length=n+1)
for (i in 1:n){
  x=(day[i]-105)/10
  if (x>0) bB[i]=0.125*(x/1.93)^0.52*exp(-x/1.93)/(1.93*0.887)
}

mB=0.0012
alphaB=0.182
gammaB=0.667
nuB=0.3

NMmin=1.0
pM=1.0
pB=0.125

betaM=seq(0, n); betaM=k*pM
betaB=seq(0, n); betaB=k*pB


# initialisation

LM=seq(0.001, 0.001, length=n+1)
SM=seq(5, 5, length=n+1)
EM=seq(0, 0, length=n+1)
IM=seq(0.01, 0.01, length=n+1)
NM=seq(5.01, 5.01, length=n+1)
```

```
SB=seq(1, 1, length=n+1)
EB=seq(0, 0, length=n+1)
IB=seq(0, 0, length=n+1)
RB=seq(0, 0, length=n+1)
DB=seq(0, 0, length=n+1)
NB=seq(1, 1, length=n+1)


# epidemic model

for (i in 1:n){
  lambdaB=dM[i]*betaB[i]*IB[i]/KB
  lambdaM=dM[i]*betaM[i]*IM[i]/KB

  LM[i+1]=LM[i] + (bL[i]*dM[i]*NM[i]-mL[i]*LM[i])*(1-LM[i]/KM)-bM[i]*LM[i]
  SM[i+1]=SM[i] - lambdaB*SM[i]+bM[i]*LM[i]-mM[i]*SM[i]
  EM[i+1]=EM[i] + lambdaB*SM[i]-gammaM[i]*EM[i]-mM[i]*EM[i]
  IM[i+1]=IM[i] + gammaM[i]*EM[i]-mM[i]*IM[i]
  NM[i+1]=SM[i+1]+EM[i+1]+IM[i+1]
  if (NM[i+1]<NMmin) {SM[i+1]=SM[i]; EM[i+1]=EM[i]; IM[i+1]=IM[i]}

  SB[i+1]=SB[i] + (bB[i]-(bB[i]-mB)*NB[i]/KB)*NB[i]-lambdaM*SB[i]-mB*SB[i]
  EB[i+1]=EB[i] + lambdaM*SB[i]-gammaB*EB[i]-mB*EB[i]
  IB[i+1]=IB[i] + gammaB*EB[i]-alphaB*IB[i]-mB*IB[i]
  RB[i+1]=RB[i] + (1-nuB)*alphaB*IB[i]-mB*RB[i]
  DB[i+1]=DB[i] + nuB*alphaB*IB[i]
  NB[i+1]=SB[i+1]+EB[i+1]+IB[i+1]+RB[i+1]
}


# output graphics

plot (t/365, LM, type="l", xlim=c(0,n/365), ylim=c(0, 120), xlab="time (years)",
ylab="mosquitoes", lty=2, lwd=1.5)
lines(t/365, SM, lty=1, lwd=1.5)
abline(h=100, lty=4); text(4.5, 108, "KM")
plot (t/365, IM, type="l", xlim=c(0,n/365), ylim=c(0, 3), xlab="time (years)",
ylab="mosquitoes", lty=1, lwd=1.5)

plot (t/365, SB, type="l", xlim=c(0,n/365), ylim=c(0, 1), xlab="time (years)", ylab="birds",
lty=2, lwd=1.5)
lines(t/365, RB, lty=3, lwd=1.5)
lines(t/365, NB, lty=1, lwd=1.5)

plot (t/365, IB, type="l", xlim=c(0,n/365), ylim=c(0, 0.25), xlab="time (years)",
ylab="birds", lty=1, lwd=1.5)
```

See also: http://epidemic-modeling.vetmeduni.ac.at/usuvmodel.htm